



Error study of rail/wheel point contact method for moving trains with rail roughness

S.H. Ju *, J.R. Liao

Department of Civil Engineering, National Cheng-Kung University, Tainan City, Taiwan, ROC

ARTICLE INFO

Article history:

Received 28 August 2009

Accepted 1 April 2010

Available online 10 May 2010

Keywords:

Contact

Field measurement

Finite element analysis

Ground vibration

Rail irregularity

Train

ABSTRACT

This study investigates the accuracy of the point contact scheme for trains moving on rails with irregularities. The advantages of this scheme are that it requires only linear analysis, a coarse mesh, and low CPU time. Two validations were performed. The first one compared this method with the surface contact method that models the actual wheel–rail contact behavior. Finite element results indicate that the two schemes almost produce identical results. The second validation used field measurements to study the accuracy of the point contact scheme applied to train–rail–bridge problems. The comparison indicates that finite element analyses are acceptably accurate.

© 2010 Elsevier Ltd. All rights reserved.

1. Introduction

The contact behavior between the wheel of moving trains and the rail with irregularities is complicated. To accurately model this problem using the finite element method, a very fine mesh with appropriate contact scheme between the wheel and rail should be generated. However, this approach is not suitable for modeling a whole train and rail system especially with the soil profile, because there are too many degrees of freedom, and also rail irregularities are difficult to model in detail. For this reason, people often use a simplified point contact model to simulate this problem, but the accuracy of this scheme is always doubted. Thus, this study investigates the accuracy of the point contact scheme by comparing it with the surface contact method that models the actual wheel–rail contact behavior. Many studies have discussed the simulation of wheel–rail contact problems with rail irregularities, and the review of these researches can be found in Ref. [1]. However, few studies have discussed simulation accuracy. Igeland studied the influence of different track parameters on the dynamic contact force between a rolling wheel and a rail. Track parameters were estimated from in-field measurements of dynamic flexibilities at a selected test site. Comparisons between calculated and measured wheel/rail contact forces at the test site were made [2]. Xia et al. studied the problem of vehicle–bridge dynamic interaction system under articulated high-speed trains, and the proposed analysis model and the solution method are then verified through the comparison between the calculated results and the in situ measured

data [3]. Auersch presented an integrated model for the computation of vehicle–track interaction and the ground vibrations of passing trains and used a combined finite element and boundary element method to calculate the dynamic compliance of the track on realistic soil with multi-body models for the vehicle. The theoretical methods were proven by experiments in several respects and at several instances [4]. Xia and Zhang investigated the dynamic interaction between high-speed trains and bridges by theoretical analysis and field experiments. The bridge was modeled using the modal superposition technique, and the measured track irregularities were taken as the system excitation [5]. Zhang et al. studied the dynamic interaction between a high-speed train and simply supported girders by theoretical analysis and field experiments, and established the dynamic interaction model of the train–bridge system. The measured track irregularities were taken as the system excitation [6]. Nielsen simulated vertical vehicle–track interaction at frequencies of 20–2000 Hz, and measured the results from two field test campaigns to validate the vehicle–track interaction model [7]. Most of the above Refs. [1–6] used the point contact schemes. Since it is widely adopted in the numerical and theoretical methods, an accuracy study of this method is necessary.

2. Formulation of the rail irregularity used in this study

Rail irregularities are a major source of vibration for moving trains. A sample function $r_v(X)$ of the rail irregularity [8] is used in this study

$$r_v(X) = \sum_{k=1}^N a_k \cos(\omega_k X + \phi_k) \quad (1)$$

* Corresponding author. Tel.: +886 6 2757575/63119; fax: +886 6 2358542.
E-mail address: juju@mail.ncku.edu.tw (S.H. Ju).

Table 1
Rail irregularity parameters used in the numerical analyses.

A_r (m ² rad/m)	ω_1 (rad/m)	ω_2 (rad/m)	ω_l (rad/m)	ω_u (rad/m)	N
0.8×10^{-7}	0	1	0.08	20	1000

where a_k is the amplitude, ω_k is a frequency (rad/s) within the upper and lower limits of the frequency $[\omega_l, \omega_u]$, ϕ_k is a random phase angle in the interval $[0, 2\pi]$, X is the global coordinate in the rail direction, and N is the total number of terms. The parameters a_k and ω_k are computed respectively by:

$$a_k = 2\sqrt{G_{rr}(\omega_k)\Delta\omega}, \quad \omega_k = \omega_l + (k-1/2)\Delta\omega, \quad \text{and} \quad \Delta\omega = (\omega_u - \omega_l)/N, \quad k = 1, 2, \dots, N \quad (2)$$

$$G_{rr}(\omega) = \frac{A_r \omega_2^2 (\omega^2 + \omega_1^2)}{\omega^4 (\omega^2 + \omega_2^2)} \quad (3)$$

where $G_{rr}(\omega)$ is a power spectral density (PSD) function, A_r is the roughness coefficient, and ω_1 and ω_2 are frequencies that change the shape of $G_{rr}(\omega)$. If ω_1 is set to zero, Eq. (3) is the same as the power spectral density function in Ref. [9]. Thus, only ω_2 and A_r are required in Eq. (3). If ω is smaller than ω_2 , $G_{rr}(\omega)$ is approximately proportional to $1/\omega^2$; otherwise $G_{rr}(\omega)$ is approximately proportional to $1/\omega^4$.

In this paper, we performed field measurements and finite element analyses of a high-speed train running in the south of Taiwan for comparison. The rail irregularity had an amplitude of 2 mm per 20 m of the rail in the vertical and transverse directions of the rail, and irregularity parameters are shown in Table 1. Fig. 1a shows the vertical PSD from the field measurements and simulation. The measured PSD was obtained using the actual rail vertical coordinate along the rail direction, and the simulation was calculated using Eq. (3) with the data in Table 1. This figure indicates that the data in Table 1 are good enough to simulate the rail irregularity near the location of our field experiments. Fig. 1b shows the vertical rail irregularity profile from the simulation. The transverse rail irregularity is similar to the vertical one near our experimental region, so the data in Table 1 was used for both directions. For a train speed of 300 km/h using the data of Table 1, frequencies ω_l and ω_u equal to 0.08 and 20 rad/m, respectively, specify that the actual vibration frequencies covered a broad range between 1 and 265 Hz. Frequency ω_2 of 1 rad/m means that the major part

of vibration (frequency < 20 Hz) is approximately proportional to $1/\omega^2$.

3. Point and surface contact methods for moving wheels

3.1. Point contact method

In this study, we set the rail direction in the global X-direction and the negative gravity direction in the global Z-direction. If another coordinate system is set, a transformation should be used. The wheel element contains a stiffness k_r between the rail and wheel, in which the stiffness k_r can be set to be in the X-, Y-, or Z-direction [10]. If the two target nodes and the wheel node are nodes 1, 3, and 2 respectively, the 3-node element stiffness for the nodal displacements $(X_1, \theta_1, X_2, X_3, \theta_3)$ is:

$$\mathbf{S} = \mathbf{T}^T \begin{bmatrix} k_r & -k_r \\ -k_r & k_r \end{bmatrix} \mathbf{T}, \quad \mathbf{T} = \begin{bmatrix} 0 & 0 & 1 & 0 & 0 \\ N_1 & N_2 & 0 & N_3 & N_4 \end{bmatrix}, \quad (4)$$

where X_1, θ_1, X_3 , and θ_3 are the translations and rotations at target nodes 1 and 3, respectively, X_2 is the translation of the wheel node, and N_i represents the cubic Hermitian interpolation functions. The load F including all the trainload on the wheel is in equilibrium with the system, so this load F on node 2 should be transformed into nodes 1 and 3 to obtain the force vector \mathbf{f} as follows:

$$\mathbf{f}^T = [N_1 \quad N_2 \quad 0 \quad N_3 \quad N_4] F \quad (5)$$

The irregularity between the rail and wheel can be easily included. Only the element forces \mathbf{f}_r are required to add into the global force vector as follows:

$$\mathbf{f}_r^T = [N_1 \quad N_2 \quad -1 \quad N_3 \quad N_4] k_r r_v(X) \quad (6)$$

where $r_v(X)$ is a function of the rail irregularity, such as that of Eq. (1), and X is the wheel location in the moving wheel direction (X-axis). For Hertzian contact theory, k_r can be approximated as follows [11]:

$$k_r = k_H \Delta_H^{1/2} \quad (7)$$

where Δ_H is the deformation between the wheel and rail, and k_H is the constant Hertzian stiffness. Thus, Eq. (7) produces a nonlinear finite element analysis. To avoid this inconvenience, a constant k_r with a considerably large value can be set to neglect the Δ_H effect. This is reasonable, since Δ_H is often very small compared to the rail

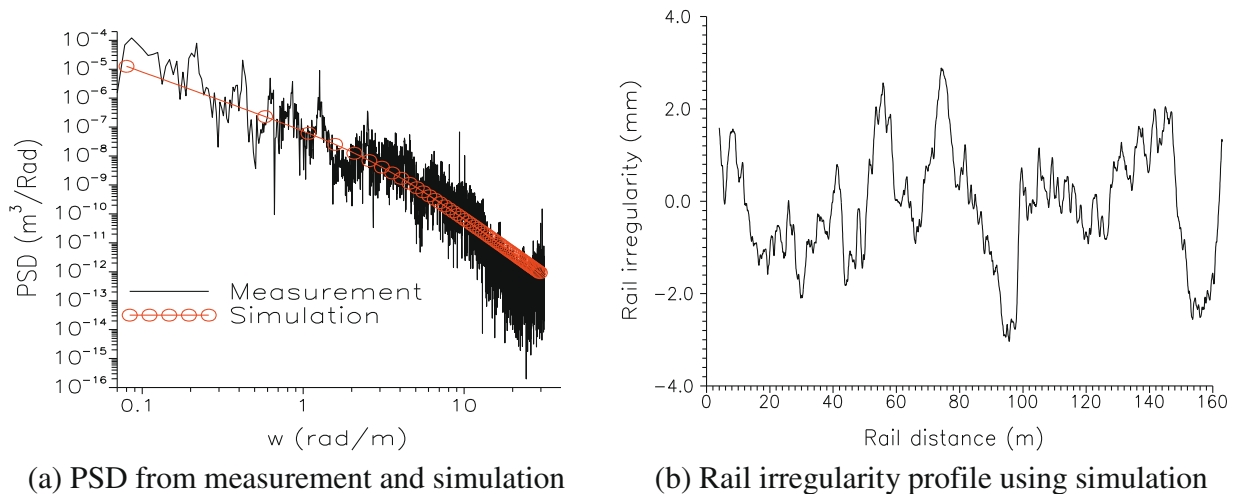


Fig. 1. Illustration of vertical rail irregularity data used in this study (data in Table 1 were used to obtain the simulation results, and the measured PSD was calculated from the rail vertical coordinate along the rail direction).

Download English Version:

<https://daneshyari.com/en/article/510155>

Download Persian Version:

<https://daneshyari.com/article/510155>

[Daneshyari.com](https://daneshyari.com)